Eur. Phys. J. A (2025) 61:103
https://doi.org/10.1140/epja/s10050-025-01530-8

THE EUROPEAN PHYSICAL JOURNAL A

Review

Clustering in nuclei and hadrons

Atsushi Hosaka[1,2,a], **Yoshiko Kanada-En'yo**[3,b], **Yasuhiro Yamaguchi**[4,5,6,c]

[1] Research Center for Nuclear Physics, Osaka University, Ibaraki, Osaka 567-0047, Japan
[2] Advanced Science Research Center, Japan Atomic Energy Agency, Tokai, Ibaraki 319-1195, Japan
[3] Department of Physics, Kyoto University, Kyoto 606-8502, Japan
[4] Department of Physics, Nagoya University, Nagoya 464-8602, Japan
[5] Kobayashi-Maskawa Institute for the Origin of Particles and the Universe, Nagoya University, Nagoya 464-8602, Japan
[6] Meson Science Laboratory, Cluster for Pioneering Research, RIKEN, Wako, Saitama 351-0198, Japan

Received: 6 November 2024 / Accepted: 1 March 2025

Communicated by Maria Borge

Abstract Clustering phenomena in hadron and nuclear systems are overviewed. Because the energy scales for hadron and nuclear systems are not very much different, we can apply similar ideas and methods for the study of the seemingly different two systems, with the key ingredient, cluster. Once clusters are formed, they develop low lying excitations near the threshold if suitable interaction is available. This is a universal phenomenon which has been known as the threshold-rule. For nuclear systems the most established is the alpha (α-)cluster which is the nucleus of ^{4}He. How the α-clusters develop in nuclei of light-medium mass region, typically ^{12}C is discussed in a microscopic manner based on the antisymmetrized molecular dynamics. The evidences of such clustering in some static properties of nuclei and scattering phenomena are discussed. Similar clustering phenomena occur for hadrons, where quark clusters are developed in either colored or colorless channels which are considered to play an important role for exotic hadrons of multi-quarks. In particular colorless hadronic clusters can be good constituents to form molecular-like structure near threshold regions.

1 Introduction

1.1 Formation of clusters and hierarchies of matter

Cluster formation is considered as another phase of matter as well as the three familiar bulk phases with uniformity such as gas, liquid and solid. The latter are often regarded as infinitely extended systems. Their properties are determined in principle by constituents' interactions and, if available, external parameters such as temperature or densities.

The systems that we discuss here are nuclei as nuclear many-body systems and hadrons as quark many-body systems. They are the ingredients of more than 99% in mass of the visible matter, atomic nuclei which are finitely extended systems. As we will see below, for many nuclei and hadrons, cluster structure emerges and dominates the properties of the systems. This is the issue that we discuss here.

Clusters are systems of finite number of *fundamental constituents* (in the following we often refer to them simply as *constituents* as long as there is no confusion). If clusters are sufficiently stiff, they can form many-cluster systems where the clusters become constituents (effective degrees of freedom) at different levels of hierarchies of matter formation. This situation can be shown as;

- Hierarchy 1: fundamental constituents → clusters.
- Hierarchy 2: clusters as constituents → many-cluster systems (clustered matter).

Once clusters are developed, due to their heavier mass than the masses of their constituents, excitations associated with cluster motion occur at lower energies than the excitations of

Yoshiko Kanada-En'yo and Yasuhiro Yamaguchi contributed equally to this work.

[a] e-mail: hosaka@rcnp.osaka-u.ac.jp (corresponding author)
[b] e-mail: yenyo@ruby.scphys.kyoto-u.ac.jp
[c] e-mail: yamaguchi@hken.phys.nagoya-u.ac.jp

Published online: 13 May 2025

the constituents. The former could be regarded as collective excitations while the latter as single-particle excitations.

In many-cluster systems, the properties of clusters may vary from those when they are isolated. For example, if the matter density increases, the clusters start to overlap, and their identity becomes less clear. As the density becomes higher the clusters are no longer good degrees of freedom and we have to consider the dynamics of their constituents. We may say that this is a transition of the structure from one type to another, and plays an important role in understanding many nuclei and hadrons.

Microscopic treatment of such transitions is not an easy task in quantum many-body physics. However, a significant progress has been achieved in nuclear physics by having well-established interaction between nucleons owing to abundant data as well as good theories. In contrast, situation is not so easy for hadrons, because the interaction among the constituent quarks has still uncertainties. Even the properties of the constituent quarks are not well established to the extent that they can be employed for various applications. Certainly the quark model has been useful but when applied to various states especially to exotic hadrons many parameters are turned depending on the states and phenomena.[1]

1.2 Charge neutrality

Having the above remarks, in this paper, we discuss clusters in subatomic systems of femtometer scale. They are atomic nuclei formed by nucleons (protons and neutrons) and hadrons formed by quarks. In both systems, hierarchical structure emerges. A nucleus as a many-nucleon system is not necessarily a uniform system of nucleons, but may find alpha clusters that are the lumps of two protons and neutrons [1,2]. Similarly, a hadron as many-quark system may find clusters of two quarks (diquarks or mesons), three quarks (triquarks or baryons) and so on [3–5].

These clusters are not necessarily well developed, or well identified objects, as we have mentioned the case of high density matter. Such a situation with rather fragile clusters can be (at least approximately well) described by the *coexistence* of different types of structures.

In nuclear physics this has been discussed by the reduced width amplitude and its integrated value (so-called spectroscopic factor) [6] and in hadron physics compositeness [7–12]. This strategy is particularly useful in understanding the structures of many-body systems. We will emphasize the importance of the coexistence in the works discussed in this paper.

In the formation of clusters, the concept of charge neutrality is important. A well known example is an atom, which is a bound system of a positively charged nucleus and negatively charged electrons. The nucleus and electrons interact attractively via electromagnetic interaction, forming charge-neutral atoms. They are regarded as the clusters of a nucleus and electrons. The interaction between neutral atoms is weaker than the original Coulomb force, and exists as the van der Waals force. (As a matter of triviality, the interaction between clusters must be weaker than the interaction between their constituents; If the inter-cluster force is too strong, clusters cannot keep their form in many-cluster systems.) This may form another hierarchy of matter, a many-cluster system.

Similar structure emerges for nuclear and hadron systems. Nucleons interact via the nuclear force. The main component of the force is spin and isospin independent central force. Yet spin and/or isospin dependent force plays important roles. Main part of such a force is driven by the exchange of Yukawa's pion between nucleons. The pions are (virtually) created and annihilated by spin and isospin dependent sources (charges), just like photons are created and annihilated by electric charge. The spin and isospin dependence may lead to the concept of spin and isospin saturation; (iso)spin up nucleon and (iso) spin down nucleon may form a null-(iso)spin system by four nucleons, that is the α-cluster (helium nucleus). The resulting α-clusters interact relatively weakly and may form new structures as collections of α-clusters. Another candidate, though not as clear as the α-cluster, is the dineutron (nn). To clarify the nature of the dineutron clusters (correlations) is important for neutron rich matter such as neutron rich nuclei and dense nuclear matter, for instance, in the core of neutron stars.

For hadrons, their constituents, quarks and gluons, interact via exchange of gluons, which depends on their color and spin. Due the *strong* color-dependent force, color neutral systems are the most tightly bound forming hadrons which may become constituents of multi-hadron systems. One of the recent subjects is on exotic hadrons, some of which may emerge as such multi-hadron systems, referred to as hadronic molecule [13,14]. Relatively weak, but not negligible spin-dependent force may lead to spin-neutral diquark systems. They could be loosely bound but could become effective constituents of hadrons. The relevance of the diquarks for hadron structure has been discussed for both light and heavy hadrons. Light diquarks are expected to be well developed in heavy baryons such as charmed (cqq) and bottomed (bqq) baryons.[2] Furthermore, heavy diquarks such as cc or bb can be also developed due to the strong color-electric force in doubly heavy baryons and tetraquarks [15,16].

[1] The most fundamental theory is Quantum Chromodynamics (QCD). Quarks and gluons there are *bare* But for low energy hadron systems, the constituent quarks and gluons play as quasi-particles of QCD. The quarks we discuss here are the latter ones as we briefly discuss in Sect. 3.

[2] Here in this paper, q denotes up (u) and down (d) quarks, and Q charm (c) quark and bottom (b) quark.

1.3 Scope of this paper

The purpose of this paper is to report a part of research outputs from nuclear and hadron physics achieved in the project "Clustering as a window on the hierarchical structure of quantum matter" with some new materials.[3] As anticipated in the previous subsections, these two systems have been developed as different fields. Today, however, we have realized similar aspects and the study in one system can be useful to the other system in both conceptual and technical points of view.

Historically, the importance of the cluster dynamics was recognized by the idea of the threshold-rule [2] for molecular states of alpha clusters (nuclei). Since then phenomenological cluster theories were developed in various manner, but then recently ab-initio methods have become available due to the developments of computational tools and methods [1,17]. Clustering phenomena has reached at the microscopic and quantitative level for atomic nuclei. In these years, various experimental researches to confirm cluster structures and discover new cluster states have been performed based on nuclear reaction analyses such as inelastic scattering and knock-out reactions (for example, references [18–20]).

Independent of these developments in nuclear physics, hadronic molecule was conjectured immediately after the discovery of the charm quark [21]. Almost 30 years after that the first candidate of hadronic molecule was observed, the $X(3872)$. Since then many other candidates have been observed at LHCb, Belle, BESIII, and so on. Yet, we have not reached satisfactory understanding of these states. For example, it is not yet very clear what are the fundamental (or effective) constituents. However, for $X(3872)$ there are good amount of evidences as a hadronic molecule of $D\bar{D}^*$ mesons. The idea has expanded to a great amount, having resulted in many studies.[4] Perhaps it is fair to say that the study of hadronic systems is still at a phenomenological level, while efforts are made for various microscopic methods, using effective field theories, lattice simulations and so on. In doing so, the idea and technique developed for atomic nuclei should become useful in one way or another. In particular, the technique in nuclear reactions as mentioned above can be used in hadron physics.

[3] Supported by Grant-in-Aid for Scientific Research on Innovative Area.

[4] Some of recent review articles are [22–24] and references therein.

2 Clustering in nuclei

2.1 Coexistence of independent particles and α-clusters

A nucleus is a finite quantum many-body system of protons and neutrons, which form a self-bound system via the attractive nuclear forces. An important aspect of the nuclear system is coexistence of two different natures, the independent-particle (mean field) feature and the cluster (a subunit formed by spatially correlated nucleons) feature. Because of the coexistence, rich phenomena appear in nuclear systems depending on the proton and neutron numbers, energy, and density. It is known that various nuclear phenomena can be dominantly described by the independent-particle picture in a mean field, nevertheless, the cluster feature often appears even in the ground state as the ground state correlation. Once a cluster is formed by correlating nucleons at the nuclear surface, the inter-cluster motion can be easily excited with a small amount of energy, and developed cluster structures appear in excited states. ^{12}C is a typical example of cluster and mean-field coexisting systems. The ground state $^{12}\mathrm{C}(0^+_1)$ is a mean-field (shell-model-like) state dominated by the $p_{3/2}$-subshell closed configuration but it contains significant mixing of 3α-cluster component. Namely, α clusters are partially formed in the ground state of ^{12}C. In excited states such as the $^{12}\mathrm{C}(0^+_2)$ and $^{12}\mathrm{C}(3^-_1)$ states, spatially developed 3α-cluster structures appear [1].

In light stable nuclei, the excitation energies of such cluster states are several MeV at most because of the saturation property of nuclear binding energy. The energy cost for the cluster excitation is comparable to single-particle excitation energies. As a result, different kinds of excitation modes appear in the low-energy region: one is the single-particle excitation and the other is the inter-cluster excitation. The energy systematic of developed cluster states can be roughly understood by the threshold rule so-called Ikeda diagram [2], which predicts developed cluster structures in energy regions near the corresponding cluster-decay threshold energies and successfully describes appearance of the 2α-cluster, 3α-cluster, and ^{12}C+α-cluster structures in ^{8}Be, ^{12}C*, and ^{16}O*.

In light neutron-rich nuclei, a further rich phenomena are expected to appear in excited states because of excess neutrons surrounding clusters (see references in Ref. [25]). An example, which has been intensively investigated by many groups, is the cluster structure in neutron-rich Be having valence neutrons around a 2α-cluster core. The cluster feature of neutron-rich Carbon and Oxygen isotopes is also a challenging topic to be investigated.

To clarify the cluster feature and discover new cluster states, various experimental attempts such as the α breakup, α resonant scattering, and α-transfer reactions have been performed. In recent studies of cluster states, researches of isoscalar monopole (ISM) and dipole (ISD) excitations have

been proceeding remarkably through α inelastic scattering experiments because the ISM and ISD operators strongly excite the inter-cluster motion [26,27].

In the theoretical side, systematic study of various cluster phenomena in stable and unstable nuclei is necessary for comprehensive understanding of nuclear systems. For this aim, we need a theoretical framework that can describe various cluster phenomena including cluster formation/breaking in the ground and inter-cluster modes in excited states in general nuclei. We applied a method of antisymmetrized molecular dynamics called AMD and its extended versions [25,28] to structure calculations and also utilized the obtained result for the microscopic reaction calculations. In the following sections, we discuss some recent researches of cluster phenomena in light nuclei based on AMD calculations.

2.2 Low-energy monopole and dipole modes in neutron-rich Oxygen

As mentioned previously, investigation of the isoscalar monopole (ISM) and dipole (ISD) excitations with α inelastic scattering have been intensively performed in these decades. Since the ISM and ISD operators can directly excite inter-cluster motions, they are good probes for cluster states, which can be found in the low-energy (LE) monopole and dipole strengths decoupling from high-energy strengths for the giant resonances as discussed in Refs. [26,27] for such $Z = N$ stable nuclei as ^{16}O and ^{24}Mg.

Another picture to understand the low-energy ISD strengths is the toroidal dipole (TD) mode (called also the torus or vortical mode), which was originally proposed with hydrodynamical models in 1980's (see Refs. [29,30] and references). The TD mode carries vorticity and conserves the nuclear density, and therefore, its energy is expected to be lower than that of high-lying IS giant dipole resonance which is considered to be a compressive dipole mode of the collective motion. For neutron-rich nuclei, also the low-energy isovector-type dipole ($E1$) modes have been attracting a great interest as a new-type of excitation mode in association with astrophysical interest (see related reviews, for example, Ref. [31]). The low-energy $E1$ strengths are often called as pigmy dipole resonances (PDR) and associated with a surface neutron oscillation against a core (neutron-skin mode or pigmy dipole resonances).

Recently, the $E1$ and isoscalar dipole (ISD) transition strengths of low-lying 1^- states of ^{20}O were measured by inelastic scattering experiments [32]. The experiment reported different properties between the 1^-_1 and 1^-_2 states for the $E1$ and ISD strengths and suggested existence of different types of low-energy dipole (LED) modes in ^{20}O. We investigated LED excitations in ^{16}O, ^{18}O, and ^{20}O using a AMD method—variation after K-projection (K-VAP) in the framework of β-constraint AMD combined with the generator coordinate method (GCM)— which was developed for the study of LED excitations [33–35].

Figure 1 shows the theoretical energy spectra of the $0^+_{1,2}$ and $1^-_{1,2}$ states in ^{16}O, ^{18}O, and ^{20}O. The TD mode was obtained as the lowest 1^-_1 state in ^{16}O, ^{18}O, and ^{20}O. However, the low-energy $E1$ mode was found only in the ^{20}O(1^-_2) state but not in the ^{16}O and ^{18}O systems. This result indicates that the low-energy $E1$ mode is an LED excitation peculiar to neutron-rich systems that does not appear in stable Oxygen isotopes near the $N = Z$ line, whereas the TD (vortical) mode is a LED excitation that generally appears in the stable and unstable regions of light nuclei. In addition to the TD mode, the cluster mode containing the C+α cluster structure was obtained in ^{16}O and ^{18}O as the 1^-_2 states, which construct the parity-doublet $K^\pi = 0^-$ bands of the positive-parity $K^\pi = 0^+$ cluster bands. In the case of ^{20}O, the parity-doublet cluster bands were theoretically predicted in the energy region higher than the TD and $E1$-type LED modes. The appearance of the high-lying cluster bands in ^{20}O can be understood by the threshold rule as the α-decay threshold energy in ^{20}O is higher than those in ^{16}O and ^{18}O because two clusters (C and α) are bound more tightly by valence neutrons.

The calculated transition current densities are shown in Fig. 2. In the $0^+_1 \to 1^-_1$ transition, the vortical flow of the proton current density is induced by the one-proton excitation as shown in Fig. 2a and describes the TD nature. In contrast, the $0^+_1 \to 1^-_2$ transition shows a translational flow along the deformed (Z) axis contributing the $E1$ strength rather than a vortical flow (see Fig. 2b).

2.3 Cluster states probed by proton and α inelastic scattering

To experimentally confirm the clustering in the ground and excited states of stable nuclei, various attempts have been performed by utilizing α-transfer and α-resonant scattering reactions to extract the α probability (so called the α spectroscopic factor or the reduced width amplitude).

An alternative way that can be applicable also to unstable nuclei is the α inelastic scattering reaction. Recently, the (α, α') reaction has been applied to search for new cluster states near the threshold in light stable nuclei such as ^{11}B, ^{12}C, ^{16}O, ^{24}Mg, and ^{32}S [26,36]. Since the α inelastic scattering is sensitive to the transition strengths, it can strongly populate excited states with clustering, in particular, 0^+ states, via remarkable monopole transitions to cluster states.

In ^{12}C, 3α cluster states near the threshold energy have been extensively investigated from astrophysical interest. Not only the 0^+_2 state but also other cluster states have been suggested to contribute to the reaction rate in stellar nucleosynthesis. To search for new cluster states, ^{12}C(α, α') reac-

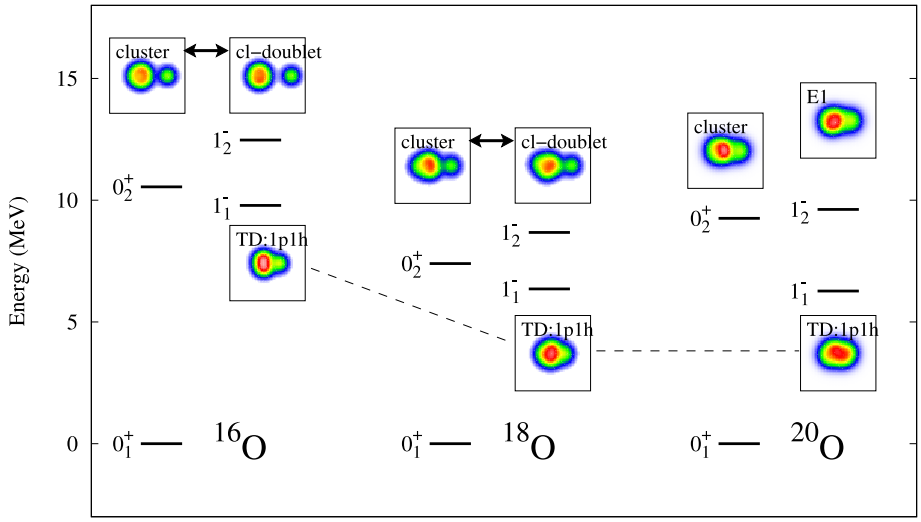

Fig. 1 Energy spectra of the $0^+_{1,2}$ and $1^-_{1,2}$ states in ^{16}O, ^{18}O, and ^{20}O calculated with the β-constraint AMD framework combined with the K-projection and generator coordinate method. For excited states, intrinsic matter densities of the dominant bases are also shown with labels "TD:1p1h", "cluster", "cluster-doublet", and "E1", which indicate the TD:toroidal dipole mode, $K^\pi = 0^+$ cluster state, its parity doublet $K^\pi = 0^-$ state, and the $E1$(electric dipole) mode, respectively. For ^{20}O, the cluster and cluster-doublet states are obtained in the higher energy ($E_x > 17$ MeV) region. The theoretical(experimental) values of the α-decay threshold energies in ^{16}O, ^{18}O, and ^{20}O are 11.2 (7.14) MeV, 6.3 (6.22) MeV, and 16.4 (12.31) MeV, respectively. Figures are taken from Ref. [35]

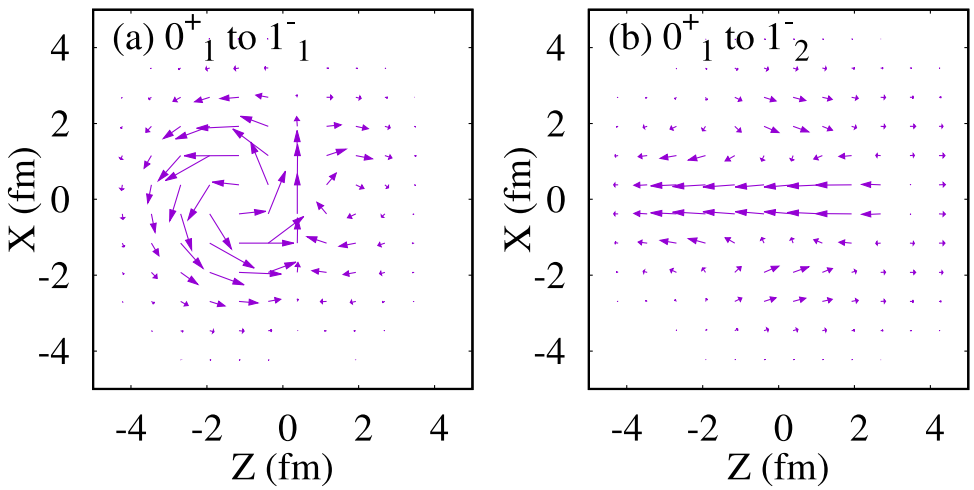

Fig. 2 Isovector component of the current densities corresponding to **a** the $0^+_1 \to 1^-_1$ and **b** the $0^+_1 \to 1^-_2$ transitions of ^{20}O. Figures are taken from Ref. [35]

tion experiments have been performed, and 0^+ and 2^+ states have been newly discovered a few MeV above the 3α threshold energy [38]. However, properties of these states have bot been clarified yet.

For study of the cluster structures of ^{12}C, the ^{12}C(α, α') reaction has been investigated in details with reaction models, but many of the reaction calculations encountered a severe overshooting problem of the ^{12}C(0^+_2) cross section, called "missing monopole strength". This was a crucial problem in the study of cluster states with the α inelastic scattering (see Ref. [39] and references therein). Minomo and Ogata overcome this problem: they applied the g-matrix folding model using the transition densities of a cluster model of ^{12}C, and succeeded to reproduce the measured 0^+_2 cross sections [41].

We applied the g-matrix folding model to the ^{12}C(α, α') reaction using the ^{12}C transition densities obtained by the structure calculation of AMD. Namely, the α inelastic scattering off ^{12}C has been investigated with the coupled-channel (CC) calculation using α-nucleus optical potentials, which were microscopically derived by folding the Melbourne g-matrix NN interaction with densities of ^{12}C obtained by the AMD method combined with the 3α generator coordinate method (AMD+GCM).

The micrsocopic CC calculation reproduces the observed cross sections of α inelastic scattering off ^{12}C at incident energies of $E_\alpha = 130$–386 MeV for various excited states of ^{12}C such as the $0^+_{2,3}$, $2^+_{1,2}$, and 3^-_1 states. In Fig. 3, calculated

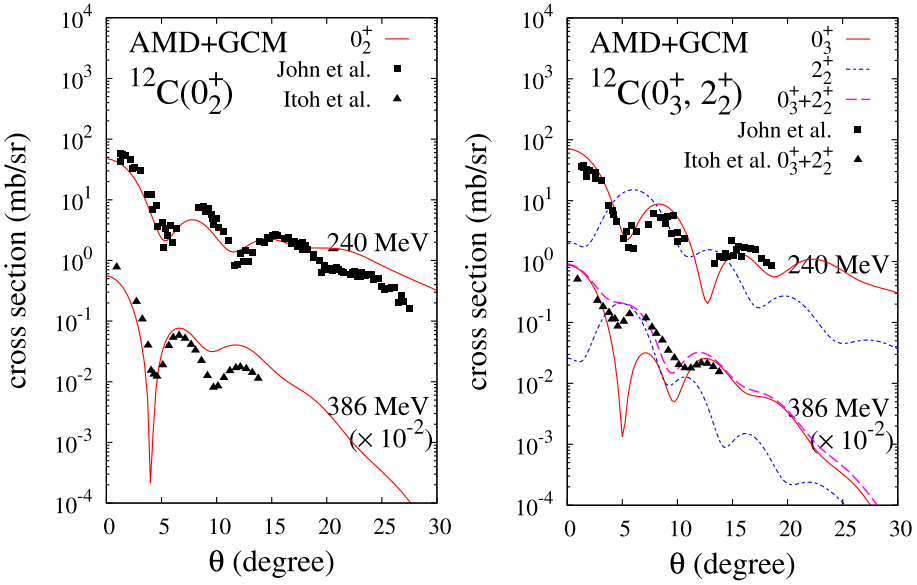

Fig. 3 The α scattering cross sections off ^{12}C at $E_\alpha = 240$ MeV, and 386 MeV ($\times 10^{-2}$) (left) for the 0^+_2 state and (right) those for the 2^+_2 and 0^+_3 states obtained by the CC calculation with the AMD+GCM compared with the experimental data [37–39]. For the cross sections at 386 MeV, the sum of the 2^+_2 and 0^+_3 cross sections is compared with data containing the 2^+_2(9.84) MeV and 0^+_3(9.93 MeV) states [38]. The figures are reproduced from the original figure of Ref. [40]

cross sections of the $0^+_{2,3}$ and 2^+_2 states near the threshold energy are shown in comparison with the experimental data. For the monopole transitions to the 0^+_2 state, the calculation reproduces well the amplitudes of the first and second peaks. It should be noted that there is no overshooting problem of the 0^+_2 cross sections without adjustable parameters in the reaction model in the present microscopic CC calculation. This successful reproduction indicates that the present method is a powerful approach to extract information of excited states from inelastic α scattering reaction.

The right panel of Fig. 3 shows the cross sections of the 0^+_3 and 2^+_2 states. These states at 9–10 MeV attracts an astrophysical interest as they may give non-negligible contribution to the triple-α reaction rate at high temperature. The 0^+_3 cross sections at $E_\alpha = 240$ MeV [37] are reasonably reproduced by the calculation with the AMD+GCM which gives the monopole strength $B(E0) = 10\,\mathrm{e^2fm^6}$ for the $0^+_1 \to 0^+_3$ transition. For the 2^+_2 state, which was newly discovered by the (α, α') experiments, incoherent sum of the 2^+_2 and 0^+_3 cross sections at 386 MeV are compared with the experimental sum of the 2^+_2(9.84) MeV and 0^+_3(9.93 MeV) [38]. In the result, the calculated 0^+_3 cross sections describe the first peak of the experimental sum and the 2^+_2 contributes to the second peak. The good agreement with the inelastic cross section data supports reliability of the model inputs in the present calculation for unknown strengths of the $E0$, $E2$, and $E3$ transitions.

Also for ^{16}O, the experimental studies by means of ^{16}O(α, α') reaction have been performed to investigate cluster states near the threshold energy [39,45]. However, in experimental analysis, a similar overshooting problem of the 0^+ cross sections has been reported [39]. In the structure studies of ^{16}O, a variety of cluster structures such as the 4α-tetrahedral, ^{12}C+α, and a 4α-cluster gas state have been suggested by cluster model and AMD calculations (see references in Refs. [43,46]).

In the recent experimental studies [39,45], the ^{16}O(α, α') cross sections were analyzed with a reaction model using phenomenological CC potentials to investigate cluster structures of excited 0^+ states. However, there are few microscopic CC calculation of the ^{16}O(α, α'), mainly because of theoretical difficulties of microscopic structure models in description of ^{16}O.

We applied the g-matrix folding model to the ^{16}O(α, α') reaction in a similar way to the ^{12}C(α, α') reaction [43]). For the structure inputs from the microscopic calculation of ^{16}O, we adopted the matter and transition densities calculated with a vertion of AMD (VAP:variaton after spin-parity projection) combined with the GCM [46]. It should be noted that the present calculation is the first microscopic CC calculation of the ^{16}O(α, α') reaction that is based on the microscopic α-nucleus CC potentials derived with the g-matrix folding model. The result reproduces well the observed elastic and inelastic cross sections of the $0^+_{1,2,3,4}$, 2^+_1, 1^-_1, and 3^-_1 states at incident energies of $E_\alpha = 104$ MeV, 130 MeV, 146 MeV, and 386 MeV.

Figure 4a, b show the (α, α') cross sections to the excited 0^+ states obtained by the CC calculation compared with the experimental data. The DWBA (one-step) calculation is also shown. In general, the 0^+ cluster states with significant monopole strengths are strongly populated by the (α, α') reaction. The calculated 0^+_3 and 0^+_4 cross sections are in good agreement with the observed data, indicating that there is no overshooting problem of the 0^+ cross sections in the present calculation. Comparing with the DWBA calculation corresponding to the direct (one-step) transition without

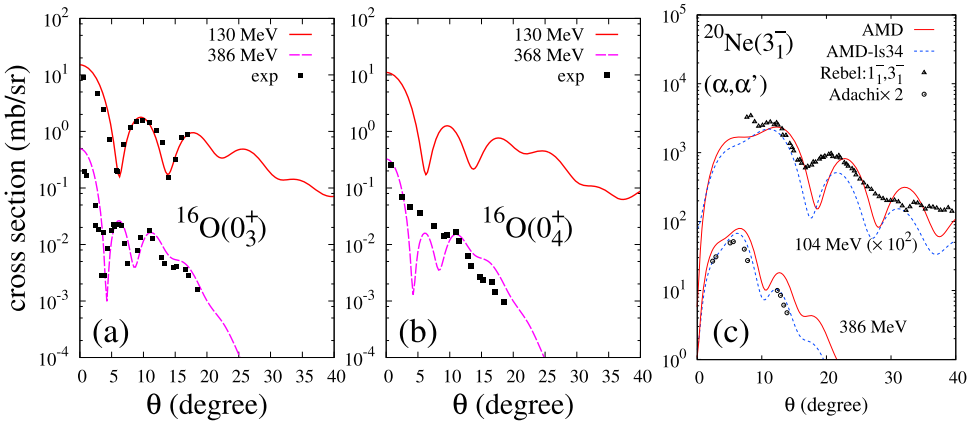

Fig. 4 **a**, **b** ^{16}O(α,α') cross sections at E_α=130 MeV and 386 MeV ($\times 10^{-2}$) for the 0^+_3 and 0^+_4 states, and **c** ^{20}Ne(α,α') cross sections at E_α = 104 and 386 MeV for the 3^-_1 state obtained by the CC calculations with the AMD, compared with the experimental data [39,42]. The ^{20}Ne(α,α') data at E_α = 104 MeV contain the 1^-_1 and 3^-_1 contributions around 5.7 MeV. The ^{20}Ne(α,α') data at 386 MeV of Ref. [39] are multiplied by a factor of two. Figures are from Refs. [43,44]

the coupled-channel effect, one can see non-negligible CC effects in the 0^+_3 and 0^+_4 cross sections, in particular, at the low incident energies, E_α = 104–146 MeV. For the 0^+_2 cross sections, we obtained further significant CC effect mainly because of the strong in-band $E2$ transition between the 0^+_2 and 2^-_1 states in the ^{12}C+α-cluster: the peak amplitude of the 0^+_2 cross sections at E_α = 104–146 MeV are largely reduced by about a factor of three from the one-step cross sections.

In the experimental studies of the monopole transitions, the monopole transition strengths are usually determined from the measured (α,α') cross sections by assuming a simple scaling law of the α-scattering cross sections and the electric monopole transition strength $B(E0)$, or based on the DWBA calculation. However, such the scaling law does not work for the cluster states as shown above in the comparison of the CC and DWBA calculations. Instead, the microscopic coupled-channel calculations are necessary to draw correct answers to the properties of monopole strengths from the (α,α') data.

^{20}Ne is an interesting system where cluster and mean-field states coexist in the low-energy region. It is known that the ^{16}O+α cluster structure appears even in the ground state of ^{20}Ne and the parity doublet partner $K^\pi = 0^-$ band exists at 5.79 MeV. The reason for the cluster structure in the ground state and low-lying $K^\pi = 0^-$ band is understood by the threshold rule: the ^{16}O+α threshold energy is only 4.73 MeV in the ^{20}Ne system meaning a small energy cost for the developed clustering. Interestingly, a $K^\pi = 2^-$ band having the mean-field aspect appears slightly below the $K^\pi = 0^-$ band.

In Ref. [44], we discussed properties of excited states by the reaction analysis of proton and α inelastic processes. A particular attention is paid on the coexistence of two kinds of negative-parity excitation modes: the mean-field and cluster components in the $3^-_1(K^\pi = 2^-)$ and $3^-_2(K^\pi = 0^-_1)$ states. Structures of ^{20}Ne were calculated with variation after parity and total angular momentum projections (VAP) in the antisymmetrized molecular dynamics(AMD). Using the obtained AMD densities of ^{20}Ne, the microscopic coupled-channel calculations of proton and α scattering off ^{20}Ne were performed with the g-matrix folding model. The calculation reasonably reproduces the observed cross sections of proton scattering at E_p = 25–35 MeV and α scattering at E_α = 104–386 MeV.

Figure 4c compares the calculated (α,α') cross sections for the 3^-_1 state with the experimental data. The labels "AMD" and "AMD-ls34" correspond to those obtained using two sets of structure inputs. The latter (AMD-ls34) case describes well the energy spectra of the $K^\pi = 2^-$ and $K^\pi = 0^-_1$ bands of ^{20}Ne. Compared to the experimental 3^-_1 cross sections at E_α = 386 MeV, the AMD-ls34 obtains a good agreement with the data, but the AMD does not. This result supports the dominant mean-field component in the $3^-_1(K^\pi = 2^-)$ state with significant mixing of the cluster component. Moreover, we performed similar reaction analysis for the (p,p') cross section, and found signatures of the mean-field and cluster components in the 3^-_1 and 3^-_2 states and significant mixing of them in the comparison with the data. It was concluded that the α and proton inelastic cross sections are good probe for the coexistence of two kinds of negative-parity bands – the $K^\pi = 2^-_1$ band with the single-particle excitation and the $K^\pi = 0^-_1$ band with the $^{16}\mathrm{O}+\alpha$ cluster structure – and the significant mixing of them.

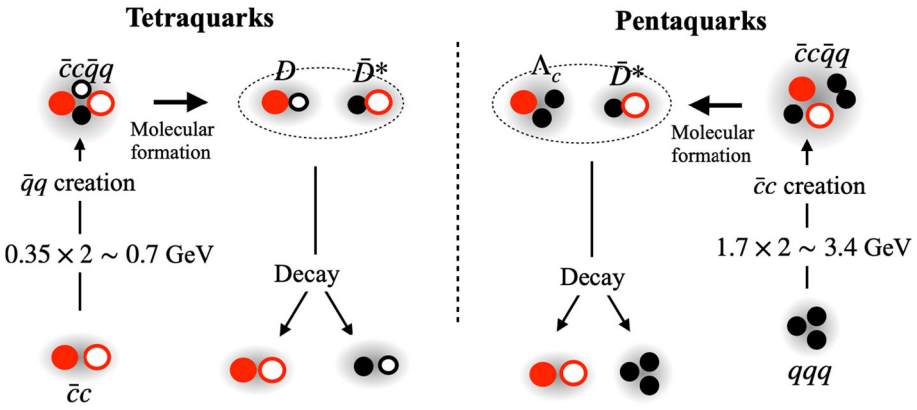

Fig. 5 Schematic picture for $\bar{q}q$ creation and the formation of molecular states of tetraquarks and pentaquarks

3 Clustering in exotic hadrons

3.1 General aspects

Hadrons are systems of quarks and gluons. They are governed by Quantum Chromodynamics (QCD) whose ingredients are the "bare" quarks and gluons. Due to the dynamics of color SU(3) gauge theory, the most relevant here is spontaneous breaking of chiral symmetry, properties of the original u, d, s quarks are modified. Most notably is the mass generation, the masses of the light bare quarks ($m_u \sim 2$ MeV, $m_d \sim 5$ MeV and $m_s \sim 90$ MeV) become heavy ($m_u \sim m_d \sim 360$ MeV, $m_s \sim 540$ MeV). The properties of heavy quarks (c, b quarks) may be also modified due to nonperturbative dynamics of QCD. For instance, the bare c quark mass is ~ 1.3 GeV, while heavier mass around 1.6 GeV is often employed for quark model calculations. In total, those massive constituent quarks play as effective degrees of freedom (or quasiparticles) of QCD dominating the properties of hadrons at low energies.

Before discussing concrete examples, let us make a rough sketch what is expected for hadrons near the threshold. As a typical case, let us consider excitations of a heavy charmonium such as $\bar{c}c$ and a hidden-charm pentaquark, $\bar{c}cqqq$. The reason that we consider the systems including heavy quark and antiquark pair is that heavy systems are more likely to be bound or resonate than light systems.

As shown by the right and left upper-arrows in Fig. 5, when sufficient amount of energy is given to the system, $\bar{q}q$ (for the charmomium) or $\bar{c}c$ (for the pentaquark) pair is created, forming a four-quark configurations $\bar{c}c\bar{q}q$, or five-quark configurations $\bar{c}cqqq$. There are several clustering possible; for instance for the tetraquarks, $[\bar{c}q]$-$[\bar{q}c]$, $[\bar{c}\bar{q}]$-$[qc]$. The former is dominated by a colorless correlation, while the latter colored correlation. Assuming a color-dependent interaction between quarks (as expected by a one-gluon exchange interaction proportional to $\lambda^a\lambda^a$ with color Gell-Mann matrices λ_a), color singlet quark pair, for instance, $\bar{c}q$ feels more attraction than $\bar{c}\bar{q}$ pair. As a consequence the colorless cluster $\bar{c}q$ is better developed and plays as a constituent, forming a molecular-like configuration, as shown in the upper middle of Fig. 5.

These molecular states can exist near the threshold region as a loosely bound or quasi-stable (resonant) state, if there is suitable attractive interaction between the colorless clusters. They are shallow, because the interaction between the colorless clusters is expected not to be as strong as colored force. The molecular structure describes essentially the properties at long distances near the threshold. What is sometimes confusing is that for such long-distance properties long-range interaction is responsible. In fact, the presence of the light quarks induces long-range pion exchanges between the colorless clusters (hadrons) which supplies attraction for the formation of shallow (quasi-)bound states. However, in addition to such a long-range interaction, a short-range interaction also becomes relevant. A short-range interaction can contribute to the formation of weakly bound or resonant states near thresholds. This requires sometimes a consideration of long-distance and short-distance dynamics simultaneously, and leads to the mixture of several configurations of different types.

This leads to the concept of the spectroscopic factor. Molecular states of hadrons, and α cluster states are not pure, in the sense that the constituent hadrons or α's may overlap and change their properties from those when they are isolated. This is well seen in Fig. 1 where clear and less clear cluster structures are shown. In general these states are written as superpositions of several states of different structure. Keeping these remarks in mind, we discuss two examples where colorless clusters are well developed, the tetraquark $X(3872)$ and pentaquarks $P_c(4312, 4440, 4457)$.

The final remark here is that molecular-like states containing heavy quark and antiquark pair are not stable and eventually decays into a pair of hadrons, one of which is a quarkonium as shown in the middle down-arrows. In the heavy quark limit, the color electric force of Coulomb type may leads to a deeply bound state as the binding energy via the $1/r$ type attraction is proportional to the heavy quark

mass. The tetraquarks and pentaquarks that we discuss below contain heavy and anti-heavy quarks and light quarks.

3.2 Tetraquark $X(3872)$

The $X(3872)$ state was first observed in 2003 by Belle in the weak decay of the B meson, $B^{\pm} \to J/\psi\, \pi^+\pi^- K^{\pm}$ [47], and was confirmed by many following experiments. In the latest PDG, the new naming χ_{c1} is employed, and the mass M and width Γ are $M = 3871.64 \pm 0.06$ MeV and $\Gamma = 1.19 \pm 0.21$ MeV [48]. The mass is very close to the sum of the masses of D^0 and $\bar{D}^{*0}$ (charge neutral) D-mesons, $m_{D^0} + m_{\bar{D}^{*0}} = (1864.84 \pm 0.065) + (2006.86 \pm 0.05) = 3871.17$ MeV. Hence $X(3872)$ is almost at the threshold of D^0 and $\bar{D}^{*0}$ mesons within the uncertainly. Due to its decay modes such as $X(3872) \to J/\psi\rho(\pi\pi)$, $J/\psi\omega(\pi\pi\pi)$ the minimal quark content of $X(3872)$ is likely to be $\bar{c}c\bar{q}q$, hence the tetraquark.[5]

The spin-parity is also known to be $J^P = 1^+$ [49,50]. These facts are consistent with that the $X(3872)$ is a near threshold S-wave state of D^0 and $\bar{D}^{*0}$. It is also important that these masses are substantially apart from the sum of the charged D^+ and $\bar{D}^{*-}$, 1869.66 ± 0.05 MeV and 2010.26 ± 0.05 MeV, respectively. The charge and neutral mass difference is 8.75 MeV, which is large in the relevant energy scale near the threshold. Because of this mass difference in the neutral and charged channels, isospin symmetry is maximally violated as seen in its decay, $X(3872) \to J/\psi\rho,\ J/\psi\omega$ [51] (we do not discuss this in detail here, except pointing out that it determines the charge conjugation of $X(3872)$ is positive).

The very proximity of the mass of $X(3872)$ to the threshold has caused discussions that $X(3872)$ could be a kinematical effect, cusp associated with opening the $D^0 D^{*0}$ channel. The cusp is a singularity where derivative of an S-wave cross section becomes discontinuous at the threshold due to the opening of a new reaction channel, where flux of the lower channel starts to escape into the new open channel, and is a consequence of probability conservation ($SS^\dagger = 1$, where S is the S-matrix). Kinematic singular effect is important, especially for hadron reactions where there many reaction channels are involved. The experimental data shows a very sharp peak in the invariant mass distribution for $X(3872)$. If there is no (or only week) interaction between D^0 and $\bar{D}^{*0}$, it is difficult to explain such a sharp peak structure. Therefore, a reasonable question is what interactions are available in the reaction channels. A shallow bound state near a threshold can easily turns into a virtual state (and vise versa), by a small change in the attraction. Such an example is in the two-nucleon system; spin-zero pn state holds a virtual state near the pn threshold, while there is a shallow bound state for spin-one pn channel that is the deuteron.

Having said this much, we discuss an admixture model for $X(3872)$.[6] The model space is spanned by molecular channels formed by $D\bar{D}^*$, $D^*\bar{D}^*$ and states other than them. As discussed in the previous subsection, the molecular channels describe long-distance properties, while the states other than that is for the short-distance dynamics. In this regard, this description differs from many works of (pure) molecular picture. In Refs. [14,52], the non-molecular component was assumed to be $\bar{c}c$ but not necessarily specified to it; it can be any that are not described by the molecular components as long as it is of short-distance nature. The total wave function for $X(3872)$ is expanded with coefficients c's as

$$\begin{aligned}
&\Psi = c_{c\bar{c}}|c\bar{c}\rangle + |\psi_0\rangle + |\psi_\pm\rangle,\\
&|\psi_{0,\pm}\rangle = c_{0,\pm}(^3S)|D\bar{D}^*(^3S_1)\rangle + c_{0,\pm}(^3D)|D\bar{D}^*(^3D_1)\rangle\\
&\qquad\qquad + c_{0,\pm}(^5D)|D^*\bar{D}^*(^5D_1)\rangle, \qquad (1)
\end{aligned}$$

where the lower indices in the coefficients c's, $0, \pm$, indicate charges of channels. The first term, $|c\bar{c}\rangle$, is for short-distance and the rest, $|\psi_0\rangle + |\psi_\pm\rangle$ for long-distance properties. The wave function Ψ has the spin parity $J^P = 1^+$ and positive charge conjugation. The $D^*\bar{D}^*$ components are included because in the heavy quark limit D and D^* mesons become degenerate and their mixing will be important.

The Hamiltonian takes a matrix form whose components are labeled by the components of the model space. In Ref. [14], the important part of the interaction between the D and D^* mesons is provided by the one pion exchange potential (OPEP). This is expected if we consider quark components of D and D^* mesons as $\bar{c}q$ (or $\bar{q}c$). With broken chiral symmetry, the constituent quarks $q \sim u, d$ couples with the Nambu-Goldstone boson, the pion. The structure of the coupling is determined, and the strength which is dictated by the axial coupling constant of the constituent quarks is also determined by the decay $D^* \to D\pi$.

An important observation is that the OPEP has the tensor structure, $S_{12}(\hat{r}) = 3\boldsymbol{\sigma}_1\cdot\hat{r}\boldsymbol{\sigma}_2\cdot\hat{r} - \boldsymbol{\sigma}_1\cdot\boldsymbol{\sigma}_2$, that mixes different angular momentum states, $\Delta L = 2$. For the states near the threshold region the dominant partial wave is the S-wave. However due to the tensor force, the coupling to the D-wave is important (SD coupling). As is well known for the deuteron, the D-wave component of rather small mixing rate $\sim$ a few % causes non-negligible amount of attraction to form a bound state in the spin zero (isospin one) channel. In contrast, due

[5] $D(\bar{D})$ meson is formed by $c\bar{q}$ ($\bar{c}q$) quarks and has spin 0, so is a pseudoscalar meson. The quark content of $D^*(\bar{D}^*)$ meson is also the same but has spin 1, so is a vector meson. In the following we use the notation $D\bar{D}^*$ for the wave function of $X(3872)$, but actual structure is a linear combination of $\bar{D}D^*$ to guarantee proper charge conjugation quantum number.

[6] There are many articles that reviews theories of $X(3872)$. Here however, let us allow to cite two of them [13,14].

Table 1 Probabilities of various components of $X(3872)$

$\lvert c_{c\bar{c}}\rvert^2$	$\lvert c_0(^3S)\rvert^2$	$\lvert c_0(^3D)\rvert^2$	$\lvert c_0(^5D)\rvert^2$	$\lvert c_\pm(^3S)\rvert^2$	$\lvert c_\pm(^3D)\rvert^2$	$\lvert c_\pm(^5D)\rvert^2$
0.059	0.869	0.002	0.001	0.065	0.002	0.001

the absence of the tensor force in the spin one channel, there is no bound state in that channel, but a virtual state.

After the diagonalization of the Hamiltonian, it turned out that the OPEP alone was not strong enough to support a bound state near the threshold region. There could be another source of attraction, coupling of the $D\bar{D}^*$ channels to $\bar{c}c$ channel (channel other than $D\bar{D}^*$). A nearby $c\bar{c}$ state with the same quantum numbers as $X(3872)$ is $\chi_{c1}(2P)$, which has not yet been observed experimentally but was predicted by the quark model in Ref. [53]. According to the quark model, the predicted mass of $\chi_{c1}(2P)$ lies approximately 80 MeV above the $D\bar{D}^*$ threshold. Thus, the coupling is expected to generate attraction. In Ref. [14], this was the motivation to introduce the s-channel interaction through $\bar{c}c$ in addition to the t-channel OPEP for $D\bar{D}^*$. The coupling parameters can be turned to reproduce the mass of $X(3872)$. Details of how the Hamiltonian is constructed is found in Ref. [14]. Here we present some important results.

- The binding energy was fixed at $E_B = 0.16$ MeV measured from the $D^0\bar{D}^{*0}$ threshold. If measured from $D^+\bar{D}^{*-}$ threshold, it is 8.91 MeV. This is a very shallow state and many properties are universally determined, the so-called unitary limit [54]. There are, however, unique features that are characterized by coupled channels.
- In Table 1, probabilities of various components in $X(3872)$ are tabulated. The dominant component is the neutral channel $D^0\bar{D}^{*0}$ whose probability is almost 90%. This indicates that the $X(3872)$ has a structure of molecular dominance, and furthermore violation of isospin; if isospin symmetry is well satisfied, $D^0\bar{D}^{*0}$ and $D^+\bar{D}^{*-}$ mix equally. The probabilities of other components are rather small but there are some for the charged channel $D^+\bar{D}^{*-}$ and $\bar{c}c$, both of which are about 6%.
- The admixture of $\bar{c}c$ component, though its probability is small, plays an important role in providing attraction to form the shallow bound state. This small mixing rate seems consistent with the rather large production rate of $X(3872)$ at large energy pp collisions (~ 8 TeV) [55].
- The wave functions for the neutral and charged channels are significantly different as shown in Fig. 6 where dominant components of $^3S_1$ are plotted. The neutral $D^0\bar{D}^{*0}$ channel extends as far as 8.36 fm while the charged channel $D^+\bar{D}^{*-}$ 1.59 fm. These values are consistent with the relation of the binding energy and radius in the weakly bound limit, $\langle r^2\rangle^{1/2} = 1/(2\sqrt{\mu E_B})$, where μ is the reduced mass.

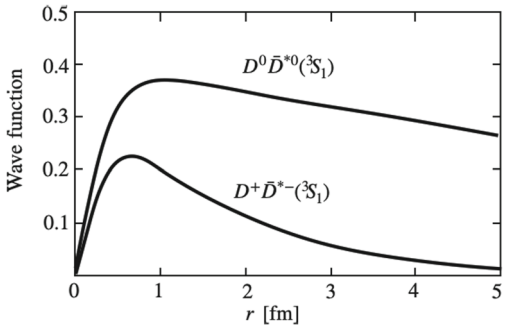

Fig. 6 Wave functions of $^3S_1$ components of $D\bar{D}^*$ channels [14]

Having made the above observations Fig. 7 shows a schematic picture for the structure of $X(3872)$.

To summarize shortly, $X(3872)$ is very likely to be a tetraquark state where four quarks $\bar{c}c\bar{q}q$ correlates and forms hadronic clusters $D\bar{D}^*$ which interact attractively such that they generate a near threshold state. The $D^0\bar{D}^{*0}$ channel causes the threshold cusp, which is enhanced or modified to a shallow bound state. Rather than asking whether the signal is for the bound or virtual state, an important question is to clarify the origin and nature of the interaction.

3.3 Pentaquarks P_c's

Pentaquark baryons have longer history as a candidate of non-standard hadrons, beyond qqq baryons. It was already reported in 1959 when Dalitz and Tuan analyzed $\bar{K}N$ scattering and implied that the hyperon resonance which is now called $\Lambda(1405)$ could be a $\bar{K}N$ molecular state [56]. Because the kaon is heavier than the pion the system is more chance to form a $\bar{K}N$ molecular-like structure than, for instance, πN systems. There are also suggestions that there is a strong attraction in isospin zero $\bar{K}N$ channel in effective models [57] and chiral models [58–61]. Recent experiments also support such a picture [62].

More evident signals have been obtained by LHCb experiments for the systems containing $\bar{c}c$ pair, which are the hidden charm pentaquarks P_c's. The first observation was reported in 2015 with a peak structure in the invariant mass of $J/\psi p$ [63]. In 2019, higher statistic data was analyzed, finding three narrow peaks [64]; at 4312 MeV, 4440 MeV and 4457 MeV. They are denoted as $P_c(4312)^+$, $P_c(4440)^+$ and $P_c(4457)^+$. Interestingly these three peaks are around the open charm hadron thresholds; the higher two around the $\Sigma_c\bar{D}^*$ threshold, and the lower one around the $\Sigma_c\bar{D}$ threshold. Because

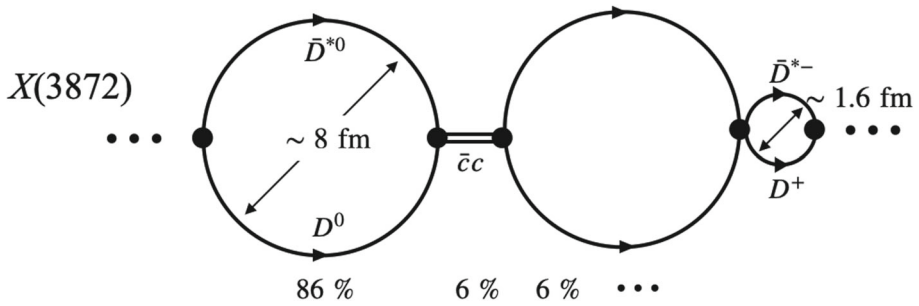

Fig. 7 Schematic picture for the structure $X(3872)$

these signals were observed in the $J/\psi p$ channel, the P_c's are considered as highly excited states of the proton, as shown on the right of Fig. 5, where together with the created $\bar{c}c$ pair, the five quarks $\bar{c}cqqq$ clusterized into $\Sigma_c\bar{D}^*$ or $\Sigma_c\bar{D}$, forming loosely bound or quasi-bound states. Because of their proximity to the thresholds, arguments of threshold singularity have been also made as cusp or triangle singularities [65,66]. As discussed in the previous subsection, a pure cusp does not develop a sharp peak while a triangle singularity may do even without a state near a threshold. Whichever the case would be, the interaction among hadrons is also important. In this paper, focusing on the role of interaction, we discuss dynamical aspect whether states are generated by a suitable interaction.

The strategy is similar to the case of the tetraquarks in the previous section. We set up a model space by a pair of hadrons that form heavy quark spin symmetry multiplets. They are $\bar{D}$ and $\bar{D}^*$ mesons, and Σ_c (spin 1/2) and Σ_c^* (spin 3/2) baryons. There is one more channel $\Lambda_c\bar{D}(\bar{D}^*)$ available. Unlike the case of $X(3872)$, there are three spin values are possible, when S-wave dominates near the threshold, $J = 1/2, 3/2, 5/2$. On the contrary the parity is fixed, negative, by assuming that the S-wave dominates. These quantum numbers are not yet confirmed experimentally, and their determination is highly important to clarify the structure of the pentaquarks.

Now the wave function is expanded just as in (1)

$$\Psi = c_{5q}|5q\rangle + c_{\Lambda_c\bar{D}^{(*)}}|\psi_{\Lambda_c\bar{D}^{(*)}}\rangle + c_{\Sigma_c^{(*)}\bar{D}^{(*)}}|\psi_{\Sigma_c^{(*)}\bar{D}^{(*)}}\rangle. \tag{2}$$

In this expression, the molecular components are denoted by ψ while $|5q\rangle$ is the component other than them. Here we do not consider isospin violation, the difference in charge combinations, as we have done for $X(3872)$. As discussed in the previous subsection, $|5q\rangle$ is supposed to be responsible for short-distance properties and ψ for long-distance properties. The molecular channels $|\psi_{\Sigma_c^{(*)}\bar{D}^{(*)}}\rangle$ are expanded by four channels, $|\psi_{\Sigma_c\bar{D}}\rangle$, $|\psi_{\Sigma_c^*\bar{D}}\rangle$, $|\psi_{\Sigma_c\bar{D}^*}\rangle$ and $|\psi_{\Sigma_c^*\bar{D}^*}\rangle$. Furthermore, S-wave dominated states are coupled by D and G-waves due to the tensor force of the OPEP. This construction of molecular channels makes the dimension of model space large; for spin 1/2 states 10 channels couple, for spin 3/2 states 15 channels, and for spin 5/2 states 16 channels [67].

The three quark structure qqq is not likely to mix for highly excited states. Therefore the states other than molecular are formed by five quarks, hence denoted as $|5q\rangle$. The $|5q\rangle$ channels are supposed to describe the short-distance dynamics. Therefore, in Ref. [67] configurations of color octet qqq and octet $\bar{c}c$ are considered. There are four independent channels for such configurations [68].

The Hamiltonian is then constructed in the matrix form with the basis components of (2). Once again the strategy is similar to the case for $X(3872)$; the interaction among the molecular channels (from the second to the fourth terms of (2)) are provided by OPEP. The interaction connecting the molecular channels and $5q$ channels is constructed by utilizing the idea of the spectroscopic factor, the overlap of the molecular channels and $5q$ channels. Details are described in Ref. [67]. The parameters for the OPEP are known as in the case of $X(3872)$. The overlap (spectroscopic factor) is also determined for all channels. Therefore, there is essentially only one unknown parameter, the overall strength (f) for the coupling between the molecular and five-quark channels. (To be fair, there is one more for the form factor for this coupling, which is however set at a typical hadronic scale of 1 GeV).

By diagonalizing the Hamiltonian we have found the pentaquark states as shown in Fig. 8. By tuning the f parameter good agreement has been obtained ($f/f_0 = 50$), not only for masses but also for widths for the observed three states $P_c(4312)$, $P_c(4440)$, $P_c(4457)$ ($P_c(4457)$ is not shown explicitly, but is in the continuum slightly above the threshold as a virtual state). Moreover, other states are predicted near the threshold regions. In addition, what is interesting and perhaps important is that for spin multiplets, 1/2 and 3/2 formed by $\Sigma_c\bar{D}^*$, and 1/2, 3/2, 5/2 formed by $\Sigma_c^*\bar{D}^*$, higher spin states appear lower than lower spin states. Moreover, the width of lower states are wider than those of higher states. This seems to contradict what we naively expect. This result is due to the tensor force of OPEP. Theoretically, when chiral symmetry is spontaneously broken and the constituent light u, d quarks couple with the pion, the OPEP should work between $\Sigma_c^{(*)}\bar{D}^{(*)}$. By now spin and parity of P_c's are not yet determined. Their determination is crucial to further clarify

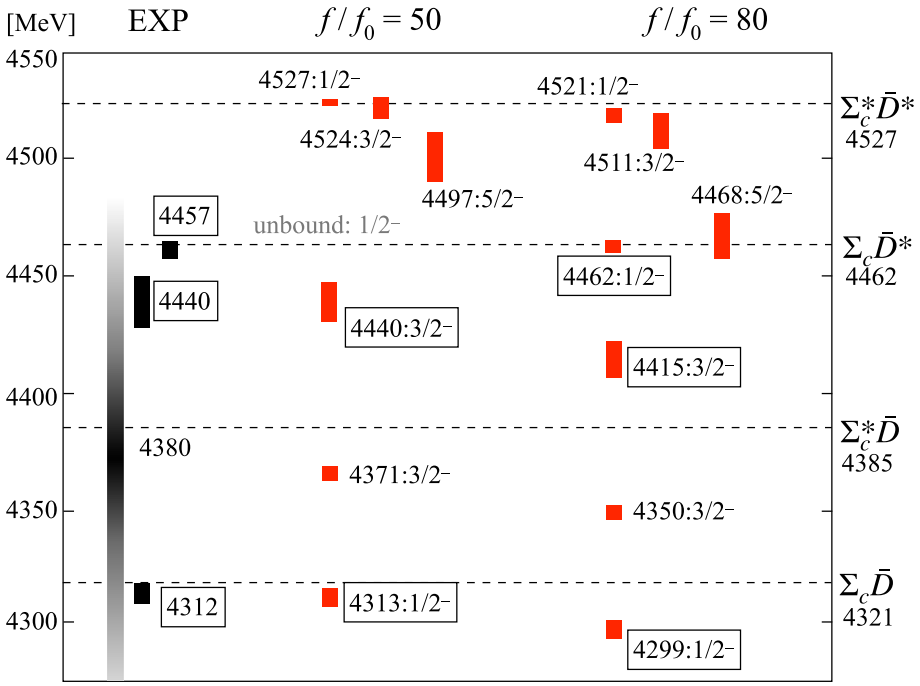

Fig. 8 Comparison of the experimental data (EXP) [63,64] (black bars) and results of the model calculation (red bars) [69]. The calculations are performed for two overall strength f. The horizontal dashed lines show the thresholds for corresponding channels and values in the right axis are isospin averaged ones in units of MeV. The centers of the bars are located at the central values of pentaquark masses while their lengths correspond to the pentaquark widths with the exception of $P_c(4380)$ width. Details are found in Ref. [69]

the nature of P_c's and the underlying dynamics that governs them.

An extended study has been performed for the pentaquakrs containing a strange quark, $\bar{c}csqq$ ($q = u, d$), motivated by the observation in 2020 [70,71]. They are $P_{cs}(4455)$ and $P_{cs}(4468)$ whose masses are 4454.9 ± 2.7 MeV and 4467.8 ± 3.7 MeV, respectively. Soon after anther signal was observed $P_{cs}(4338)$ at 4337.37 ± 0.24 MeV. The strategy is very the same as for P_c, except for (1) OPEP is supplemented by kaon exchange as the kaon is another Nambu-Goldstone boson containing a strange quark, and (2) more coupled channels are needed for expanding the P_{cs} states due to the one more flavor degree of freedom, strangeness. Once again, we refer more details to Ref. [71]. Interestingly, by using a similar value for the overall strength f to that of P_c, the observed P_{cs} states were reproduced near the thresholds. This supports the idea that the hadronic clusters are developed near the threshold region and their long-distance dynamics are dominated by the Nambu-Goldstone bosons of spontaneously broken chiral symmetry. At the same time, admixture of short-distance dynamics by the five quark components is also important both for P_c and P_{cs}. In addition to the good reproduction of the observed states, the model Hamiltonian predicts many other states near the thresholds. The abundant states of the near threshold region are indeed an realization of the conjecture made immediately after the discovery of the charm quark, rich spectroscopy near thresholds caused by the hadronic clusters and their molecules [21].

3.4 Doubly heavy hadrons

When multiquark states contain two (or more) heavy quarks qualitatively different situation may occur. Here we discuss briefly the multiquark states whose minimal quark content includes two heavy quarks. Historically theory prediction appeared long ago [72], but finer quantitative estimate was made soon after the doubly charmed Ξ_{cc} was observed [16]. Experimentally, the first signal was observed for $T_{cc} \sim cc\bar{u}\bar{d}$ [73,74].

The key ingredient for the discussion is the color electric force mediated by gluon which dominates the interaction between heavy quarks at short distances (large energy scale). This stems from the fact that the dynamics of QCD shows different faces at low and high energies as separated by the scale parameter $\Lambda_{QCD} \sim$ some hundred MeV. The dominant one-gluon exchange is the color dependent electric (Coulomb) type,

$$V(r) = \frac{g^2}{4\pi}\frac{\lambda^a\lambda_a}{r}, \tag{3}$$

where g is the quark-gluon coupling constant. A crucial fact is that the potential matrix elements are attractive both for color anti-triplet $\bar{3}_c$ for QQ system as well as for color singlet 1_c for $\bar{Q}Q$ (Q denotes a heavy quark). The strength of the $\bar{3}_c$ channel is 1/2 of that of $\bar{Q}Q$, but is strong enough for heavy quarks. A heavy quark system is essentially nonrelativistic, where the color electric force takes the potential

form of $1/r$ Coulomb type as in (3). Such a Coulomb attractive force generates a deep bound state with a binding energy as proportional to the mass of the heavy quark, M_Q. The coupling constant $\alpha_S = g^2/4\pi$ may decreases at high energies, but only logarithmically. Hence the color electric force generates a tightly bound heavy diquark.

For systems containing a heavy and anti-heavy quarks as discussed in the previous sections such a color-electric Coulomb dynamics does not appear for the formation of molecular states; they are governed dominantly by the low energy dynamics of QCD. It is relevant for the $Q\bar{Q}$ states in the decay channels. This is the reason that we expect that the molecular states containing a heavy and anti-heavy quarks cannot be absolutely stable. In other words, heavy molecular states are excited states and their corresponding ground state contains quarkonium-like state.

In contrast, for systems containing two heavy quarks, for example, $QQ\bar{q}\bar{q}$, large attraction is expected for QQ, forming a tightly bound heavy quark cluster (heavy diquark). In such a case, the would be decay channel $[Q\bar{q}]$-$[Q\bar{q}]$ receives smaller attraction of the scale Λ_{QCD}. Hence such systems may allow absolutely stable states under strong interaction decays.

To what extent the system is stable depends on the masses of heavy quarks. An estimate was done based on a finely tuned phenomenological considerations [16], which was right after the discovery of doubly charmed baryon Ξ_{cc} [75]. They predicted the mass of T_{cc} only slightly above the DD^* threshold, which agrees well with the (post-observed) data [73,74]. They also estimated other heavy tetraquarks where they have found that heavier tetraquarks, for example, T_{bb} will be very tightly bound with a binding energy nearly 200 MeV. Their estimate is supported by lattice simulations [76–80] and also by an accurate calculation for four-body systems in the quark model [72,81–84].

We note that T_{cc} has also been studied as a bound state of colorless clusters that is a hadronic molecule of DD^* [85–90], where long-range interactions play an important role to provide attractions. In such molecular states, a color 6_c configuration of the QQ system is developed rather than a color $\bar{3}_c$ one that dominates in compact $QQ\bar{q}\bar{q}$ systems [82, 91].

As an extension of doubly heavy quark system, Karliner and Rosner considered hexaquarks $[QQqqqq]$, pointing out an analogous reaction to nuclear fusion [15]. The two heavy baryons may fuse, $[Qqq]+[Qqq] \to [[QQ][qq][qq]]$. The fuel baryons $[Qqq]$ are formed by an interaction of order Λ_{QCD} while the heavy diquark $[QQ]$ in the fused hexaquark $[[QQ][qq][qq]]$ received stronger binding. Thus the fusion may occur by releasing, for bottomed system with bb, as large as a few hundred MeV. Of course, this does not seem practically useful because large energy is needed to prepare the fuel system of $[Qqq]$. It is, however, amusing to consider various processes which are provided by the formation of various kinds of clusters in multiquark systems which are possible due to multi-faces of QCD dynamics depending on energy scales and various quantum numbers, including flavors.

4 Summary and prospects

In this paper we have overviewed activities in the study of cluster dynamics for nuclear and hadron (especially exotic hadrons) systems. While they have been developed independently in their own sake, it is also the case that there are several features that can be shared each other.

Due to longer history in the study of nuclear systems, the ideas and methods in nuclear physics can be exported to hadron physics. The most important and universal one is the threshold rule when clusters are formed near the threshold by saturating the strong interaction between the fundamental degrees of freedom. Because the (effective) Hamiltonian for nuclear systems are well established including the nucleon interactions, recent developments of computational power accelerates microscopic ab-initio calculations. Also scattering experiments as well as theories have explored observation of α-cluster structures by breakup, resonant and transfer processes. These have been discussed in Sect. 2 in this paper. Recently, it is discussed that knockout reactions can be a good tool to directly observe the formation or existence of the α-clusters in nuclear structures [92]. Furthermore, seemingly less fragile clusters such as dineutron nn and deuteron pn clusters have been also discussed and studied experimentally [93,94].

The above strategies to explore cluster dynamics could, in principle, be applied to (exotic) hadrons, although there are several issues that must be challenged. The most critical is that some clusters in hadrons are colored, and cannot be isolated. When picked up the colored clusters must be accompanied by another anti-colored element to form a colorless object. This, however, is not the case for molecular states where colorless hadrons are their constituents.

Another difficulty is the fact that almost all exotic states are resonances whose lifetimes are very short of order femtometer. At this moment, it is impossible to prepare them as a target in the standard scattering experiments. Yet, we could consider a transfer-like reaction as shown in Fig. 9. A projectile virtually splits into two hadrons (for example $\pi \to D\bar{D}^*$) at vertex 1, one of the split hadron is transferred to the target hadron forming a resonant hadron at vertex 2, and finally the resonance decays into final state particles at vertex 3. This is one of examples that is planned by using high momentum pion beam at J-PARC [95]. By studying the amplitude at vertex 2 at various momentum transfer, we may be able to extract the information of spatial extension

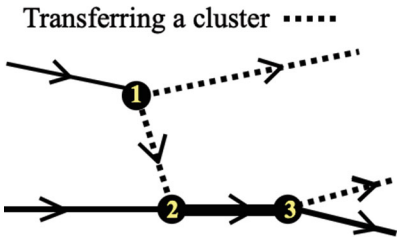

Fig. 9 A sketch of a transfer reaction. For details, see text

of the resonance, which could be information of resonance structure of molecular-like or not.

Clusters in atomic nuclei have been studied well in both theory and experiments from the middle of 20th century. In contrast, studies of clusters in hadrons have started in the 21st century. While this paper discussed the two systems, cluster dynamics shares common and universal aspects in various quantum systems such as atomic and molecular systems. Developments in various fields will stimulates each other to further open new findings in individual field.

Acknowledgements YY and AH thank S. Takeuchi, M. Takizawa, E. Santopinto, A. Giachino for the discussions of tetraquarks and pentaquarks. Discussions with K. Yoshida was useful which gave us a hint in applying nuclear reactions to hadron reactions. This work was supported in part by Grants-in Aid for Scientific Research on Innovative Areas (No. 18H05407), Grants-in-Aid of the Japan Society for the Promotion of Science (Grant nos. JP18K03617,22K03633(YK), JP20K14478 (YY)) and the RCNP Collaboration Research Network program as the project number COREnet-056 (YY).

Funding Open Access funding provided by The University of Osaka.

Data Availability Statement This manuscript has no associated data. [Authors' comment: Data sharing not applicable to this article as no datasets were generated or analysed during the current study.]

Code Availability Statement This manuscript has no associated code/software. [Authors' comment: Code/Software sharing not applicable to this article as no code/software was generated or analysed during the current study.]

References

1. M. Freer, H. Horiuchi, Y. Kanada-En'yo, D. Lee, U.-G. Meißner, Microscopic clustering in light nuclei. Rev. Mod. Phys. **90**(3), 035004 (2018). https://doi.org/10.1103/RevModPhys.90.035004. arXiv:1705.06192 [nucl-th]
2. K. Ikeda, H. Horiuchi, N. Takigawa, The systematic structure-change into the molecule-like structures in the self-conjugate 4n nuclei. Prog. Theor. Phys. Suppl. Extra Numb. **68**, 464 (1968). https://doi.org/10.1143/PTPS.E68.464
3. M. Gell-Mann, A schematic model of baryons and mesons. Phys. Lett. **8**, 214–215 (1964). https://doi.org/10.1016/S0031-9163(64)92001-3
4. G. Zweig, An SU(3) model for strong interaction symmetry and its breaking. Version 1 (1964). https://doi.org/10.17181/CERN-TH-401
5. G. Zweig, In: Lichtenberg, D.B., Rosen, S.P. (eds.) An SU(3) model for strong interaction symmetry and its breaking. Version 2, pp. 22–101 (1964). https://doi.org/10.17181/CERN-TH-412
6. H. Horiuchi, Kernels of GCM, RGM and OCM and Their Calculational Methods
7. S. Weinberg, Elementary particle theory of composite particles. Phys. Rev. **130**, 776–783 (1963). https://doi.org/10.1103/PhysRev.130.776
8. S. Weinberg, Evidence that the deuteron is not an elementary particle. Phys. Rev. **137**, 672–678 (1965). https://doi.org/10.1103/PhysRev.137.B672
9. T. Hyodo, Structure and compositeness of hadron resonances. Int. J. Mod. Phys. A **28**, 1330045 (2013). https://doi.org/10.1142/S0217751X13300457. arXiv:1310.1176 [hep-ph]
10. H. Nagahiro, A. Hosaka, Composite and elementary nature of a resonance in the σ model. Phys. Rev. C **88**(5), 055203 (2013). https://doi.org/10.1103/PhysRevC.88.055203. arXiv:1307.2031 [hep-ph]
11. H. Nagahiro, A. Hosaka, Elementarity of composite systems. Phys. Rev. C **90**(6), 065201 (2014). https://doi.org/10.1103/PhysRevC.90.065201. arXiv:1406.3684 [hep-ph]
12. T. Sekihara, T. Hyodo, D. Jido, Comprehensive analysis of the wave function of a hadronic resonance and its compositeness. PTEP 2015, 063–04 (2015). https://doi.org/10.1093/ptep/ptv081
13. A. Hosaka, T. Iijima, K. Miyabayashi, Y. Sakai, S. Yasui, Exotic hadrons with heavy flavors: X, Y, Z, and related states. PTEP **2016**(6), 062–01 (2016). https://doi.org/10.1093/ptep/ptw045. arXiv:1603.09229 [hep-ph]
14. Y. Yamaguchi, A. Hosaka, S. Takeuchi, M. Takizawa, Heavy hadronic molecules with pion exchange and quark core couplings: a guide for practitioners. J. Phys. G **47**(5), 053001 (2020). https://doi.org/10.1088/1361-6471/ab72b0. arXiv:1908.08790 [hep-ph]
15. M. Karliner, J.L. Rosner, Quark-level analogue of nuclear fusion with doubly-heavy baryons. Nature **551**, 89 (2017). https://doi.org/10.1038/nature24289. arXiv:1708.02547 [hep-ph]
16. M. Karliner, J.L. Rosner, Discovery of doubly-charmed Ξ_{cc} baryon implies a stable $(bb\bar{u}\bar{d})$ tetraquark. Phys. Rev. Lett. **119**(20), 202001 (2017). https://doi.org/10.1103/PhysRevLett.119.202001. arXiv:1707.07666 [hep-ph]
17. T. Otsuka, T. Abe, T. Yoshida, Y. Tsunoda, N. Shimizu, N. Itagaki, Y. Utsuno, J. Vary, P. Maris, H. Ueno, α-Clustering in atomic nuclei from first principles with statistical learning and the Hoyle state character. Nature Commun. **13**(1), 2234 (2022). https://doi.org/10.1038/s41467-022-29582-0
18. Y. Funaki, Alpha condensate and dynamics of cluster formation. Eur. Phys. J. A **57**(1), 14 (2021). https://doi.org/10.1140/epja/s10050-020-00321-7
19. E. Vardaci, An overview of recent experimental results in nuclear cluster physics. AIP Conf. Proc. **2038**(1), 020003 (2018). https://doi.org/10.1063/1.5078822

20. P.J. Li, Validation of the Be10 ground-state molecular structure using Be10(p, pα)He6 triple differential reaction cross-section measurements. Phys. Rev. Lett. **131**(21), 212501 (2023). https://doi.org/10.1103/PhysRevLett.131.212501. arXiv:2311.13129 [nucl-ex]
21. A. De Rujula, H. Georgi, S.L. Glashow, Molecular charmonium: a new spectroscopy? Phys. Rev. Lett. **38**, 317 (1977). https://doi.org/10.1103/PhysRevLett.38.317
22. F.-K. Guo, C. Hanhart, U.-G. Meißner, Q. Wang, Q. Zhao, B.-S. Zou, Hadronic molecules. Rev. Mod. Phys. **90**(1), 015004 (2018). https://doi.org/10.1103/RevModPhys.90.015004. arXiv:1705.00141 [hep-ph]. [Erratum: Rev.Mod.Phys. 94, 029901 (2022)]
23. H.-X. Chen, W. Chen, X. Liu, S.-L. Zhu, The hidden-charm pentaquark and tetraquark states. Phys. Rept. **639**, 1–121 (2016). https://doi.org/10.1016/j.physrep.2016.05.004. arXiv:1601.02092 [hep-ph]
24. H.-X. Chen, W. Chen, X. Liu, T.G. Steele, S.-L. Zhu, Towards exotic hidden-charm pentaquarks in QCD. Phys. Rev. Lett. **115**(17), 172001 (2015). https://doi.org/10.1103/PhysRevLett.115.172001. arXiv:1507.03717 [hep-ph]
25. Y. Kanada-En'yo, M. Kimura, A. Ono, Antisymmetrized molecular dynamics and its applications to cluster phenomena. PTEP **2012**, 01–202 (2012). https://doi.org/10.1093/ptep/pts001. arXiv:1202.1864 [nucl-th]
26. T. Yamada, Y. Funaki, T. Myo, H. Horiuchi, K. Ikeda, G. Ropke, P. Schuck, A. Tohsaki, Isoscalar monopole excitations in ^{16}O: α-cluster states at low energy and mean-field-type states at higher energy. Phys. Rev. C **85**, 034315 (2012). https://doi.org/10.1103/PhysRevC.85.034315. arXiv:1110.6509 [nucl-th]
27. Y. Chiba, M. Kimura, Y. Taniguchi, Isoscalar dipole transition as a probe for asymmetric clustering. Phys. Rev. C **93**(3), 034319 (2016). https://doi.org/10.1103/PhysRevC.93.034319. arXiv:1512.08214 [nucl-th]
28. M. Kimura, T. Suhara, Y. Kanada-En'yo, Antisymmetrized molecular dynamics studies for exotic clustering phenomena in neutron-rich nuclei. Eur. Phys. J. A **52**(12), 373 (2016). https://doi.org/10.1140/epja/i2016-16373-9. arXiv:1612.09432 [nucl-th]
29. J. Kvasil, V.O. Nesterenko, W. Kleinig, P.-G. Reinhard, P. Vesely, General treatment of vortical, toroidal, and compression modes. Phys. Rev. C **84**, 034303 (2011). https://doi.org/10.1103/PhysRevC.84.034303. arXiv:1105.0837 [nucl-th]
30. A. Repko, P.-G. Reinhard, V.O. Nesterenko, J. Kvasil, Toroidal nature of the low-energy $E1$ mode. Phys. Rev. C **87**(2), 024305 (2013). https://doi.org/10.1103/PhysRevC.87.024305. arXiv:1212.2088 [nucl-th]
31. A. Bracco, F.C.L. Crespi, E.G. Lanza, Gamma decay of pygmy states from inelastic scattering of ions. Eur. Phys. J. A **51**(8), 99 (2015). https://doi.org/10.1140/epja/i2015-15099-6
32. N. Nakatsuka, Observation of isoscalar and isovector dipole excitations in neutron-rich 20 O. Phys. Lett. B **768**, 387–392 (2017). https://doi.org/10.1016/j.physletb.2017.03.017
33. Y. Shikata, Y. Kanada-En'yo, Variation after K-projection in antisymmetrized molecular dynamics for low-energy dipole excitations in ^{10}Be and ^{16}O. PTEP **2020**(7), 073–01 (2020). https://doi.org/10.1093/ptep/ptaa092. arXiv:2003.01362 [nucl-th]
34. Y. Shikata, Y. Kanada-En'yo, Low-energy dipole excitation mode in ^{18}O with antisymmetrized molecular dynamics. Phys. Rev. C **103**(3), 034312 (2021). https://doi.org/10.1103/PhysRevC.103.034312. arXiv:2011.00821 [nucl-th]
35. Y. Shikata, Y. Kanada-En'yo, Low-energy dipole excitations in O20 with antisymmetrized molecular dynamics. Phys. Rev. C **104**(3), 034314 (2021). https://doi.org/10.1103/PhysRevC.104.034314. arXiv:2104.11400 [nucl-th]
36. Y. Chiba, M. Kimura, Cluster states and isoscalar monopole transitions of ^{24}Mg. Phys. Rev. C **91**(6), 061302 (2015). https://doi.org/10.1103/PhysRevC.91.061302. arXiv:1502.06325 [nucl-th]
37. B. John, Y. Tokimoto, Y.-W. Lui, H.L. Clark, X. Chen, D.H. Youngblood, Isoscalar electric multipole strength in C-12. Phys. Rev. C **68**, 014305 (2003). https://doi.org/10.1103/PhysRevC.68.014305
38. M. Itoh, Candidate for the 2+ excited Hoyle state at Ex 10 MeV in C-12. Phys. Rev. C **84**, 054308 (2011). https://doi.org/10.1103/PhysRevC.84.054308
39. S. Adachi, Systematic analysis of inelastic α scattering off self-conjugate A=4n nuclei. Phys. Rev. C **97**(1), 014601 (2018). https://doi.org/10.1103/PhysRevC.97.014601
40. Y. Kanada-En'yo, K. Ogata, α scattering cross sections on ^{12}C with a microscopic coupled-channels calculation. Phys. Rev. C **99**(6), 064601 (2019). https://doi.org/10.1103/PhysRevC.99.064601. arXiv:1903.10164 [nucl-th]
41. K. Minomo, K. Ogata, Consistency between the monopole strength of the Hoyle state determined by structural calculation and that extracted from reaction observables. Phys. Rev. C **93**(5), 051601 (2016). https://doi.org/10.1103/PhysRevC.93.051601. arXiv:1603.01805 [nucl-th]
42. H. Rebel, G.W. Schweimer, G. Schatz, J. Specht, R. Löhken, G. Hauser, D. Habs, H. Klewe-Nebenius, Quadrupole and hexadecapole deformation of 2s–1d shell nuclei. Nucl. Phys. A **182**, 145–173 (1972). https://doi.org/10.1016/0375-9474(72)90207-2
43. Y. Kanada-En'yo, K. Ogata, First microscopic coupled-channel calculation of α inelastic cross sections on ^{16}O. Phys. Rev. C **99**(6), 064608 (2019). https://doi.org/10.1103/PhysRevC.99.064608. arXiv:1904.03811 [nucl-th]
44. Y. Kanada-En'yo, K. Ogata, Properties of $K^\pi = 0_1^+$, $K^\pi = 2^-$, and $K^\pi = 0_1^-$ bands of ^{20}Ne probed via proton and α inelastic scattering. Phys. Rev. C **101**(6), 064308 (2020). https://doi.org/10.1103/PhysRevC.101.064308. arXiv:2003.14076 [nucl-th]
45. T. Wakasa, New candidate for an alpha cluster condensed state in O-16(alpha, alpha') at 400-MeV. Phys. Lett. B **653**, 173–177 (2007). https://doi.org/10.1016/j.physletb.2007.08.016. arXiv:nucl-ex/0611021
46. Y. Kanada-En'yo, Cluster states and monopole transitions in ^{16}O. Phys. Rev. C **89**(2), 024302 (2014). https://doi.org/10.1103/PhysRevC.89.024302. arXiv:1308.0392 [nucl-th]
47. S.K. Choi, Observation of a narrow charmonium-like state in exclusive $B^\pm \to K^\pm \pi^+ \pi^- J/\psi$ decays. Phys. Rev. Lett. **91**, 262001 (2003). https://doi.org/10.1103/PhysRevLett.91.262001. arXiv:hep-ex/0309032
48. S. Navas, Review of particle physics. Phys. Rev. D **110**(3), 030001 (2024). https://doi.org/10.1103/PhysRevD.110.030001
49. R. Aaij, Determination of the X(3872) meson quantum numbers. Phys. Rev. Lett. **110**, 222001 (2013). https://doi.org/10.1103/PhysRevLett.110.222001. arXiv:1302.6269 [hep-ex]
50. R. Aaij, Quantum numbers of the X (3872) state and orbital angular momentum in its $\rho^0 J\psi$ decay. Phys. Rev. D **92**(1), 011102 (2015). https://doi.org/10.1103/PhysRevD.92.011102. arXiv:1504.06339 [hep-ex]
51. P. Amo Sanchez, Evidence for the decay X(3872) –> J/ psi omega. Phys. Rev. D **82**, 011101 (2010). https://doi.org/10.1103/PhysRevD.82.011101. arXiv:1005.5190 [hep-ex]
52. M. Takizawa, S. Takeuchi, X(3872) as a hybrid state of charmonium and the hadronic molecule. PTEP **2013**, 093–01 (2013). https://doi.org/10.1093/ptep/ptt063. arXiv:1206.4877 [hep-ph]
53. S. Godfrey, N. Isgur, Mesons in a relativized quark model with chromodynamics. Phys. Rev. D **32**, 189–231 (1985). https://doi.org/10.1103/PhysRevD.32.189
54. P. Naidon, S. Endo, Efimov physics: a review. Rept. Prog. Phys. **80**(5), 056001 (2017). https://doi.org/10.1088/1361-6633/aa50e8. arXiv:1610.09805 [quant-ph]

55. M. Aaboud, Measurements of $\psi(2S)$ and $X(3872) \to J/\psi\pi^+\pi^-$ production in pp collisions at $\sqrt{s} = 8$ TeV with the ATLAS detector. JHEP **01**, 117 (2017). https://doi.org/10.1007/JHEP01(2017)117. arXiv:1610.09303 [hep-ex]
56. R.H. Dalitz, S.F. Tuan, A possible resonant state in pion-hyperon scattering. Phys. Rev. Lett. **2**, 425–428 (1959). https://doi.org/10.1103/PhysRevLett.2.425
57. Y. Akaishi, T. Yamazaki, Nuclear anti-K bound states in light nuclei. Phys. Rev. C **65**, 044005 (2002). https://doi.org/10.1103/PhysRevC.65.044005
58. C.G. Callan Jr., I.R. Klebanov, Bound state approach to strangeness in the Skyrme model. Nucl. Phys. B **262**, 365–382 (1985). https://doi.org/10.1016/0550-3213(85)90292-5
59. C.G. Callan Jr., K. Hornbostel, I.R. Klebanov, Baryon masses in the bound state approach to strangeness in the Skyrme model. Phys. Lett. B **202**, 269–275 (1988). https://doi.org/10.1016/0370-2693(88)90022-6
60. T. Ezoe, A. Hosaka, Kaon-Nucleon scattering states and potentials in the Skyrme model. Phys. Rev. D **96**(5), 054002 (2017). https://doi.org/10.1103/PhysRevD.96.054002. arXiv:1703.01004 [hep-ph]
61. T. Ezoe, A. Hosaka, Kaon-Nucleon systems and their interactions in the Skyrme model. Phys. Rev. D **94**(3), 034022 (2016). https://doi.org/10.1103/PhysRevD.94.034022. arXiv:1605.01203 [nucl-th]
62. S. Aikawa, Pole position of $\Lambda(1405)$ measured in d(K−, n)$\pi\Sigma$ reactions. Phys. Lett. B **837**, 137637 (2023). https://doi.org/10.1016/j.physletb.2022.137637. arXiv:2209.08254 [nucl-ex]
63. R. Aaij, Observation of $J/\psi p$ resonances consistent with pentaquark states in $\Lambda_b^0 \to J/\psi K^- p$ decays. Phys. Rev. Lett. **115**, 072001 (2015). https://doi.org/10.1103/PhysRevLett.115.072001. arXiv:1507.03414 [hep-ex]
64. R. Aaij, Observation of a narrow pentaquark state, $P_c(4312)^+$, and of two-peak structure of the $P_c(4450)^+$. Phys. Rev. Lett. **122**(22), 222001 (2019). https://doi.org/10.1103/PhysRevLett.122.222001. arXiv:1904.03947 [hep-ex]
65. S.X. Nakamura, $P_c(4312)^+$, $P_c(4380)^+$, and $P_c(4457)^+$ as double triangle cusps. Phys. Rev. D **103**, 111503 (2021). https://doi.org/10.1103/PhysRevD.103.L111503. arXiv:2103.06817 [hep-ph]
66. S.X. Nakamura, A. Hosaka, Y. Yamaguchi, $P_c(4312)^+$ and $P_c(4337)^+$ as interfering $\Sigma_c\bar{D}$ and $\Lambda_c\bar{D}^*$ threshold cusps. Phys. Rev. D **104**(9), 091503 (2021). https://doi.org/10.1103/PhysRevD.104.L091503. arXiv:2109.15235 [hep-ph]
67. Y. Yamaguchi, A. Giachino, A. Hosaka, E. Santopinto, S. Takeuchi, M. Takizawa, Hidden-charm and bottom meson-baryon molecules coupled with five-quark states. Phys. Rev. D **96**(11), 114031 (2017). https://doi.org/10.1103/PhysRevD.96.114031. arXiv:1709.00819 [hep-ph]
68. S. Takeuchi, M. Takizawa, The hidden charm pentaquarks are the hidden color-octet uud baryons? Phys. Lett. B **764**, 254–259 (2017). https://doi.org/10.1016/j.physletb.2016.11.034. arXiv:1608.05475 [hep-ph]
69. Y. Yamaguchi, H. García-Tecocoatzi, A. Giachino, A. Hosaka, E. Santopinto, S. Takeuchi, M. Takizawa, P_c pentaquarks with chiral tensor and quark dynamics. Phys. Rev. D **101**(9), 091502 (2020). https://doi.org/10.1103/PhysRevD.101.091502. arXiv:1907.04684 [hep-ph]
70. R. Aaij, Observation of a J/$\psi\Lambda$ resonance consistent with a strange pentaquark candidate in $B- \to J/\psi\Lambda p^-$ decays. Phys. Rev. Lett. **131**(3), 031901 (2023). https://doi.org/10.1103/PhysRevLett.131.031901. arXiv:2210.10346 [hep-ex]
71. A. Giachino, A. Hosaka, E. Santopinto, S. Takeuchi, M. Takizawa, Y. Yamaguchi, Rich structure of the hidden-charm pentaquarks near threshold regions. Phys. Rev. D **108**(7), 074012 (2023). https://doi.org/10.1103/PhysRevD.108.074012. arXiv:2209.10413 [hep-ph]
72. J.P. Ader, J.M. Richard, P. Taxil, Do narrow heavy multi-quark states exist? Phys. Rev. D **25**, 2370 (1982). https://doi.org/10.1103/PhysRevD.25.2370
73. R. Aaij, Observation of an exotic narrow doubly charmed tetraquark. Nat. Phys. **18**(7), 751–754 (2022). https://doi.org/10.1038/s41567-022-01614-y. arXiv:2109.01038 [hep-ex]
74. R. Aaij, Study of the doubly charmed tetraquark T_{cc}^+. Nat. Commun. **13**(1), 3351 (2022). https://doi.org/10.1038/s41467-022-30206-w. arXiv:2109.01056 [hep-ex]
75. R. Aaij, Observation of the doubly charmed baryon Ξ_{cc}^{++}. Phys. Rev. Lett. **119**(11), 112001 (2017). https://doi.org/10.1103/PhysRevLett.119.112001. arXiv:1707.01621 [hep-ex]
76. A. Francis, R.J. Hudspith, R. Lewis, K. Maltman, Lattice prediction for deeply bound doubly heavy tetraquarks. Phys. Rev. Lett. **118**(14), 142001 (2017). https://doi.org/10.1103/PhysRevLett.118.142001. arXiv:1607.05214 [hep-lat]
77. P. Junnarkar, N. Mathur, M. Padmanath, Study of doubly heavy tetraquarks in Lattice QCD. Phys. Rev. D **99**(3), 034507 (2019). https://doi.org/10.1103/PhysRevD.99.034507. arXiv:1810.12285 [hep-lat]
78. R.J. Hudspith, B. Colquhoun, A. Francis, R. Lewis, K. Maltman, A lattice investigation of exotic tetraquark channels. Phys. Rev. D **102**, 114506 (2020). https://doi.org/10.1103/PhysRevD.102.114506. arXiv:2006.14294 [hep-lat]
79. P. Mohanta, S. Basak, Construction of $bb\bar{u}\bar{d}$ tetraquark states on lattice with NRQCD bottom and HISQ up and down quarks. Phys. Rev. D **102**(9), 094516 (2020). https://doi.org/10.1103/PhysRevD.102.094516. arXiv:2008.11146 [hep-lat]
80. L. Leskovec, S. Meinel, M. Pflaumer, M. Wagner, Lattice QCD investigation of a doubly-bottom $\bar{b}\bar{b}ud$ tetraquark with quantum numbers $I(J^P) = 0(1^+)$. Phys. Rev. D **100**(1), 014503 (2019). https://doi.org/10.1103/PhysRevD.100.014503. arXiv:1904.04197 [hep-lat]
81. J. Vijande, A. Valcarce, N. Barnea, Exotic meson-meson molecules and compact four-quark states. Phys. Rev. D **79**, 074010 (2009). https://doi.org/10.1103/PhysRevD.79.074010. arXiv:0903.2949 [hep-ph]
82. E.J. Eichten, C. Quigg, Heavy-quark symmetry implies stable heavy tetraquark mesons $Q_iQ_j\bar{q}_k\bar{q}_l$. Phys. Rev. Lett. **119**(20), 202002 (2017). https://doi.org/10.1103/PhysRevLett.119.202002. arXiv:1707.09575 [hep-ph]
83. T.F. Caramés, J. Vijande, A. Valcarce, Exotic $bc\bar{q}\bar{q}$ four-quark states. Phys. Rev. D **99**(1), 014006 (2019). https://doi.org/10.1103/PhysRevD.99.014006. arXiv:1812.08991 [hep-ph]
84. Q. Meng, E. Hiyama, A. Hosaka, M. Oka, P. Gubler, K.U. Can, T.T. Takahashi, H.S. Zong, Stable double-heavy tetraquarks: spectrum and structure. Phys. Lett. B **814**, 136095 (2021). https://doi.org/10.1016/j.physletb.2021.136095. arXiv:2009.14493 [nucl-th]
85. N.A. Tornqvist, From the deuteron to deusons, an analysis of deuteron-like meson meson bound states. Z. Phys. C **61**, 525–537 (1994). https://doi.org/10.1007/BF01413192. arXiv:hep-ph/9310247
86. S. Ohkoda, Y. Yamaguchi, S. Yasui, K. Sudoh, A. Hosaka, Exotic mesons with double charm and bottom flavor. Phys. Rev. D **86**, 034019 (2012). https://doi.org/10.1103/PhysRevD.86.034019. arXiv:1202.0760 [hep-ph]
87. N. Li, Z.-F. Sun, X. Liu, S.-L. Zhu, Coupled-channel analysis of the possible $D^{(*)}D^{(*)}$, $\overline{B}^{(*)}\overline{B}^{(*)}$ and $D^{(*)}\overline{B}^{(*)}$ molecular states. Phys. Rev. D **88**(11), 114008 (2013). https://doi.org/10.1103/PhysRevD.88.114008. arXiv:1211.5007 [hep-ph]
88. T. Asanuma, Y. Yamaguchi, M. Harada, Analysis of DD* and $D^-(*)\Xi cc(*)$ molecule by one boson exchange model based on heavy quark symmetry. Phys. Rev. D **110**(7), 074030 (2024). https://doi.org/10.1103/PhysRevD.110.074030. arXiv:2311.04695 [hep-ph]

89. M. Sakai, Y. Yamaguchi, Analysis of Tcc and Tbb based on the hadronic molecular model and their spin multiplets. Phys. Rev. D **109**(5), 054016 (2024). https://doi.org/10.1103/PhysRevD.109.054016. arXiv:2312.08663 [hep-ph]
90. H.-X. Chen, W. Chen, X. Liu, Y.-R. Liu, S.-L. Zhu, An updated review of the new hadron states. Rept. Prog. Phys. **86**(2), 026201 (2023). https://doi.org/10.1088/1361-6633/aca3b6. arXiv:2204.02649 [hep-ph]
91. M. Tanaka, Y. Yamaguchi, M. Harada, Mass and decay width of Tccs from symmetries. Phys. Rev. D **110**(1), 016024 (2024). https://doi.org/10.1103/PhysRevD.110.016024. arXiv:2403.03548 [hep-ph]
92. K. Yoshida, J. Tanaka, α knockout reaction as a new probe for α formation in α-decay nuclei. Phys. Rev. C **106**(1), 014621 (2022). https://doi.org/10.1103/PhysRevC.106.014621. arXiv:2111.07541 [nucl-th]
93. T. Nakamura, Observation of strong low-lying E-1 strength in the two-neutron halo nucleus Li-11. Phys. Rev. Lett. **96**, 252502 (2006). https://doi.org/10.1103/PhysRevLett.96.252502
94. C. Samanta, N.S. Chant, P.G. Roos, A. Nadasen, A.A. Cowley, Discrepancy between proton and alpha induced cluster knockout reactions on O-16. Phys. Rev. C **26**, 1379–1384 (1982). https://doi.org/10.1103/PhysRevC.26.1379
95. K. Aoki, et al. Extension of the J-PARC Hadron Experimental Facility: Third White Paper (2021). arXiv:2110.04462 [nucl-ex]